FRONT SURFACE FIELD FORMATION AND DIFFUSION PROFILES FOR INDUSTRIAL INTERDIGITATED BACK CONTACT SOLAR CELLS

M. Cascant[1], D. Morecroft[1], K. Boulif [1], L. Vauche, H. Yuste[1], E.E. Bende[2], and F. J. Castaño[1].
[1]Siliken, High efficiency solar cell pilot line, R&D department, Ciudad Politécnica de la Innovación- UPV
Camino de Vera 14, 46022 Valencia, Spain.
[2]ECN Solar Energy, P.O. Box 1, NL-1755 ZG Petten, the Netherlands.

ABSTRACT: Optimization of the Front Surface Field (FSF) for IBC cells is important for passivation, lowering series resistance and reducing UV light degradation. This work presents results for optimizing the FSF diffusion from an industrial perspective, focusing on optimizing the process flow to achieve excellent FSF performance, whilst at the same time reducing the number of process steps. The ideal FSF profile is a compromise since a lightly doped deep diffusion reduces recombination losses close the cell surface where the light is captured, whilst increased doping reduces series resistance. This work investigates diffusing the FSF (1) at the beginning, (2) in the middle and (3) towards the end of the IBC process flow. The advantage of the first option is that the diffusion depth can be increased by subsequent thermal steps. However a diffusion barrier is required to protect the FSF throughout the subsequent processing, which increases the number of process steps and results in increased costs. By placing the FSF diffusion later in the process flow it is possible to simplify the process reducing the number of steps. Experimental results show excellent FSF diffusion passivation performance over 156mm, with lifetime values of over 500 µs. Simulations confirm that high current generation can be achieved with a short circuit current of over 40 mA cm-2.

Keywords: Interdigitated Back Contact (IBC), high-efficiency, silicon solar cell, n-type.

1 PURPOSE OF THE WORK-INTRODUCTION

Interdigitated Back Contact (IBC) solar cells can achieve high efficiency (>24%) since the p-n junction and metallization are on the rear side, enabling the full front side of the cell to capture light [1,-3]. Previous authors have discussed the importance of using an n+ diffused Front Surface Field (FSF) to improve front surface passivation [4-7], lower series resistance [8], and improve UV stability [9]. The surface recombination is reduced since the n+ diffusion repels minority carriers, and series resistance is reduced since the doped region acts as a parallel low resistance channel for majority carriers to reach the contacts.

While improved current collection and passivation can be achieved if the FSF is lowly doped near the surface, high doping is often needed to avoid conduction problems. A deep doping profile will also help to reduce series resistance, although the temperature and time of the process will be increased. The optimum FSF profile will also need to consider the pitch and emitter fraction of the IBC cell design as well as the conductivity of the base. Previous work has investigated different FSF profiles including error function dopant profiles (erfc) and gaussian profiles [8]. Results have shown that shallow highly-doped or deep lightly-doped profiles can achieve an acceptable blue response in combination with enhanced lateral transport.

The FSF can be formed at different stages of the process flow. A first alternative is to include the FSF diffusion at the beginning of the process flow. This would allow a drive-in of the FSF profile during subsequent diffusions, lowering surface recombination and series resistance. The disadvantage is that it is necessary to protect the FSF with diffusion barriers, increasing processing steps and cost and lowering throughput. A second alternative would be to create the FSF at a later stage, which simplifies the process flow by avoiding front diffusion barriers. A drawback is that from an industrial perspective it is difficult to obtain a lowly doped deep diffusion profile. The present work aims at assessing the industrial feasibility of placing the FSF diffusion at different stages of the IBC process flow.

Most previously reported work on FSF formation for IBC cells has been focused on small laboratory cells, while few reports exist using 156mm silicon substrates.

2 EXPERIMENTAL METHODS

The substrates were 180 micron thick n-type CZ wafers with a resistivity of 2.5 Ohm-cm and bulk lifetimes exceeding 1 ms. All experiments were carried out on symmetrical wafers that had been processed with saw damage removal, texturing and pre/post-diffusion cleaning, and the diffusions were carried out in a tube furnace. Figure 1 is a schematic diagram showing the high temperature steps of the IBC process flow, and the different process sequences tested including: FSF diffusion at the beginning of the process flow (FSF1); after the emitter and before the BSF diffusion (FSF2); after the BSF and before the emitter diffusion (FSF3); after the emitter and BSF diffusion (FSF4).
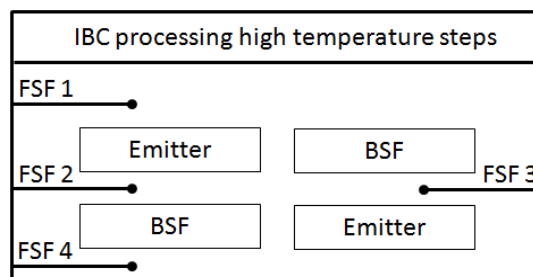

Fig. 1. Schematic diagram showing the high temperature steps of the IBC process flow, where the FSF is diffused at different stages of the process.

All of the FSF profiles tested were passivated with 20nm thick thermally grown oxide, followed by a forming gas anneal (FGA) of 450[0]C for 30 mins. Characterisation was carried out using a four-point probe to measure sheet resistance, microwave induced Photoconductive Decay (µPCD) for lifetime mapping, and Quasi-Steady-State Photoconductance (QSSPC) to measure the lifetime with

minority carrier density. Emitter saturation current density (J_{oe}) and the implied open circuit voltage ($V_{oc\ Impld}$) were also measured. Two-dimensional simulations were carried out using the simulation software MicroTec [11] to evaluate the influence of the FSF profile on the final cell parameters.

3 RESULTS

Figure 2 shows Secondary Ion Mass Spectroscopy (SIMS) profiles for FSF1- at the beginning of the process flow, and FSF4- after the BSF and emitter diffusions. A significant difference in surface doping can be observed. The doping concentration at the surface decreases from ~1×10^{20} cm^{-3} to ~5×10^{18} cm^{-3}, and the profile tends to a more Gaussian distribution. The depth of the diffusion increases from ~500 nm to ~650 nm due to the subsequent thermal steps. Processing steps after the FSF formation influence the initial doping profile, especially subsequent diffusions, surface oxidation and chemical etching.
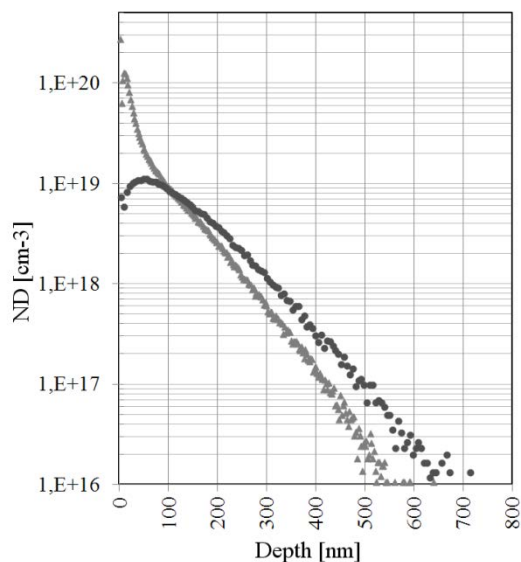

Fig. 2. Secondary Ion Mass Spectrometry (SIMS) measurements for diffusion profiles FSF1- at the beginning of the IBC process flow (grey triangles), and FSF4- after emitter and BSF diffusions (black circles).

Simulations have been carried out in order to determine the current collection of cells containing the FSF profiles depicted in Fig 2. A short circuit current density (J_{sc}) of 37,93 mA/cm^2 is obtained for the FSF1 profile while a higher J_{sc} of 38.94 mA/cm^2 is obtained for the FSF4 profile. This difference can be attributed to higher Auger recombination near the surface for doping profile FSF1.

	R_{sheet} [Ω/sqr]	J_{oe} [fA/cm^2]	$V_{oc\ limit}$ [mV]	Implied V_{oc} [mV]
FSF4	171,0	96	687	675
FSF3	145,0	43	708	685
FSF2	159,7	72	695	679
FSF1	189,6	72	695	678

Table I. A table summarizing the sheet resistance (R_{sheet}), emitter saturation current density (J_{oe}), the open circuit voltage limit $V_{oclimit}$, and implied open circuit voltage ($V_{oc\ Impld}$) for FSF diffusion profiles 1-4.
.

Table 1 summarizes the experimental results for R_{sh}, J_{oe}, $V_{oclimit}$ and $V_{ocImpld}$. Sheet resistance variations are mainly due to variations in diffusion depth. However, it is also influenced by the reduction in the surface concentration of Phosphorus. Previous work indicates that these values of sheet resistance in combination with a conductive base (< 3 Ohm-cm) can lead to a low contribution of lateral transport to series resistance [6]. Considering that the wafer doping was less than 1.8×10^{15} cm^{-3}, the dark saturation current density was calculated with the slope method as the high injection level condition was met. The values of J_{oe} and $V_{ocImpld}$ obtained indicate that the front of the cell has been effectively passivated for every process flow proposed.
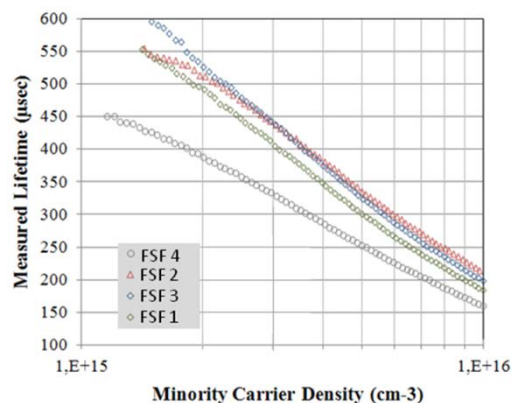

Fig. 4. Quasi-Steady-State-Photoconductance (QSSPC) measurements taken for FSF profiles 1-4.
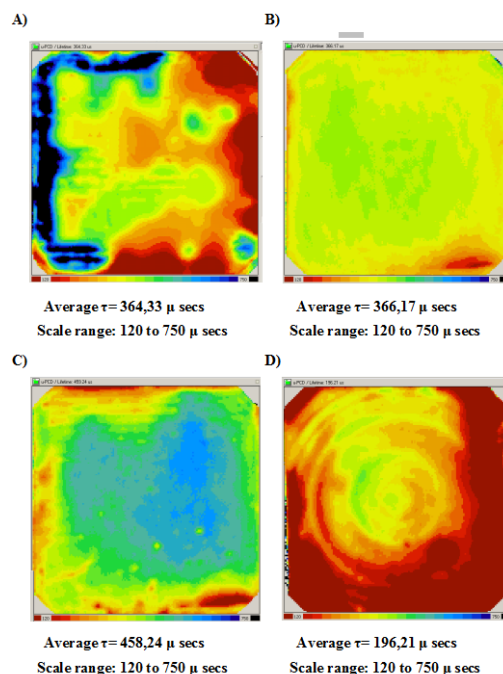

Fig. 5. Micro-photoconductance decay (μPCD) maps for A) a passivated n-type wafer without FSF, B) FSF1, C) FSF3 and D) FSF4. Shown below the images are the average lifetime, τ, and the scale range of the image in micro-seconds.

One would expect that the closer the FSF diffusion is to the beginning of the process flow, the better the passivation would be since as shown in Fig. 2, the surface is more lightly doped with a deeper diffusion profile.The results in Table 1 indicate that this is not the case, with the lowest J_o and highest $V_{oc\ Impd}$ for FSF3- placing the FSF before the emitter and after the BSF. The lifetime measurements also show the same trend, as shown in Figure 4. Average values lifetime values obtained by µPCD measurements depicted in Figure 4 show that as the number of heating steps are increased from FSF1 to FSF2 or FSF3, the lifetime increases, but then decreases significantly for FSF4. Figure 5 shows that the uniformity of the front surface passivation is much better with an FSF than without (Figs. 5A and B). Increasing the number of heating steps increases the lifetime as shown by Figs. 5B and C. FSF4 in Fig. 5D shows a significantly reduced average lifetime, and the appearance of 'rings' in the lifetime map. These rings have been previously identified as "Oxygen Induced Stacking Faults (OSF)". These defects have been traced to the seed end of the Czochralski ingot, where the interstitial oxygen concentration is the highest and the cooling rate during crystal growth is the slowest, allowing point defects to agglomerate. These stacking are known to develop during thermal processing [12]. These results indicate that it is important to consider not only the front surface passivation, but also the bulk lifetime which can be reduced by high temperature processing.

The results show that it is feasible to simplify the IBC process by diffusing the FSF at a later stage, instead of at the beginning of the process. This can help to reduce the number of diffusion protection barriers, increasing throughput and reducing cost. The results show that the bulk lifetime can be a limiting factor if the thermal budget is high. Implied V_{oc} values of 681 mV were reached under 1 sun illumination. These values indicate that an improved front surface passivation compatible with high efficiency cells has been obtained. High temperature processing of the FSF improves passivation by reducing the doping surface concentration and improving uniformity of the passivation.

Another method of reducing the front surface doping concentration is to carry out a simple etch back step, which can be achieved experimentally by a number of different methods, e.g. an alkaline/acid chemical etch, Reactive ion etching (RIE) or surface oxidation followed by an acid etch. Simulations exploring this method of enhancing front surface passivation are shown below.

4 SIMULATIONS

Simulations were carried out on IBC cell structures with 2mm pitch, 80% emitter fraction, and 75 µm gap. The diffusion profiles for the emitter, BSF and FSF1 were transferred directly from the measured SIMS profiles. Figure 6 shows how (a) the open circuit voltage (V_{oc}) and short circuit current (J_{sc}) and (b) the efficiency and fill factor change with the amount of silicon etched away from the front surface of the IBC cell. The simulations clearly indicate that a highly doped surface ($>4\times10^{19}$ dopants/cm^3) will be detrimental for J_{sc},V_{oc}, and efficiency mainly due to enhanced Auger recombination in this region. The simulations show that etching >30nm would mean a significant increase in cell performance. The fill factor decreases with increasing etch depth because the FSF is etched away, increasing the series

resistance. The simulation results indicate that it is also possible to place the FSF diffusion at the end of the IBC process flow, and include a short etch-back step to achieve good front surface passivation.
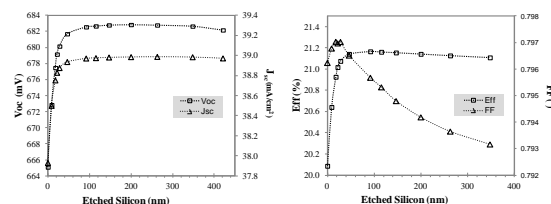

Fig. 6. Simulation results showing (a) how the open circuit voltage (V_{oc}) and short circuit current (J_{sc}) and (b) the efficiency and fill factor change with increasing silicon etch depth.

5 CONCLUSION

This work investigates the industrial feasibility of placing the FSF diffusion at different stages of the IBC cell process flow. If the FSF diffusion is placed at the beginning of the process flow, the front surface passivation can benefit from subsequent high temperature diffusions of the emitter and BSF. The high temperature steps can drive-in the surface dopants reducing Auger recombination close to the surface. The drawback of this approach is that additional diffusion protection barriers are required to protect the FSF during subsequent diffusions, increasing the number of processing steps and cost, and decreasing the throughput. The experimental results show that excellent passivation results can be achieved by placing the FSF diffusion after the BSF or emitter diffusions, thus simplifying the IBC process flow. The experimental results also indicate that it is important to take into consideration the decrease in bulk lifetime with thermal processing, due to the formation of oxygen induced stacking faults. The simulation results indicate that it may also be possible to place the FSF diffusion at the end of the IBC process flow, and include a short etch-back step. Excellent front surface passivation can be achieved by etching just the first 30 nm of silicon on the front side.

REFERENCES

[1] P. J. Cousins et al, "Gen III: Improved Performance at Lower Cost", 35th IEEE PVSC, 2010, Hawaii (USA), pp 275-277.

[2] F.J Castano et al "Industrially feasible >19% efficiency IBC cells for pilot line processing", IEEE PVSEC Seattle June 2011.

[3] M. Cascant et al "Development Towards Pilot Line Efficiency Improvements of >19% Industrially Viable IBC Solar Cells", in 26th EU-PVSEC. 2011. Hamburg (Germany).

[4] Guo, J.-H. and Cotter, J. E., "Optimizing the diffused regions of interdigitated backside buried contact solar cells". Progress in Photovoltaics: Research and Applications, 2007, 15: 211–223. doi: 10.1002/pip.730.

[6] C. Gong et al, "High Efficient N-type Interdigitated Back Contact Silicon Solar Cells with Screen-Printed Al-Alloyed Emitter", IEEE 2010

[6] F. Granek et al. "Positive Effects of Front Surface Field in High-Efficiency Back-Contact Back-Junction N-type Silicon Solar Cells", IEEE 2008

[7] F Granek *et al*, *"Front Surface Passivation of N-Type High-Efficiency Back-Junction Silicon Solar Cells using Front Surface Field"* in 22nd EU-PVSEC. 2007. Milan (Italy)

[8] F. Granek et al. "Enhanced lateral current transport via the front N+ diffused layer of n-type high-efficiency back-junction back-contact silicon solar cells", Progress in photovoltaics: research and applications, 17 (47-56) 2009

[9] F. Granek, C. Reichel, "Back-contact back-junction silicon solar cells under UV illumination", Solar Energy Materials & Solar Cells, 94, pgs 1734-1740 (2010)

[10] Granek thesis 2009

[11] User Manual Microtec 4.22, Siborg Systems Inc. From http://www.siborg.ca

[12] P. J. Cousins et al. "Generation 3: Improved Performance at lower cost", Sunpower corporation.